
Figures and figure supplements

Neural encoding of actual and imagined touch within human posterior parietal cortex

Srinivas Chivukula et al

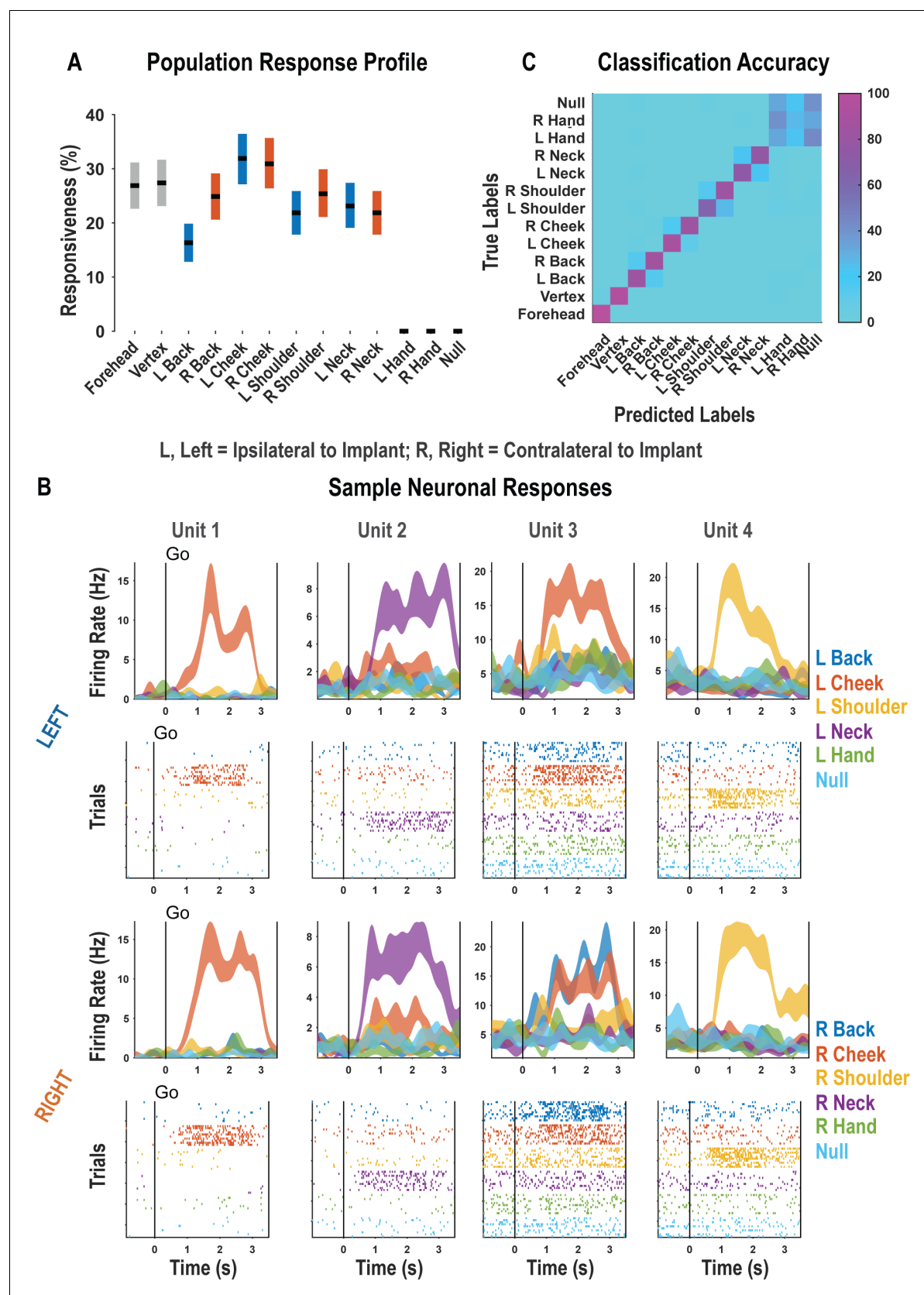


Figure 1. Postcentral-intraparietal (PC-IP) discriminably encodes bilateral tactile receptive fields. (A) Percentage of the PC-IP neuronal population that demonstrated significant modulation relative to baseline for each tested stimulation site ($p < 0.05$, false discovery rate corrected, $n = 398$ units). Results Figure 1 continued on next page

Figure 1 continued

are shown as the mean percentage (horizontal black line) of the population \pm bootstrapped 95% confidence interval (bar height). Gray bars represent truncal (midline) body locations, blue bars represent left (ipsilateral)-sided sites, and orange bars represent right (contralateral)-sided sites. Population results were pooled across recording sessions (**Figure 1—figure supplement 1**) and were not qualitatively affected by pooling together single and potential multi-units (**Figure 1—figure supplement 2**). (B) Representative neuronal responses illustrating body part discrimination. Each column of panels depicts the response for one neuron to body parts on the left (top two rows) and on the right (bottom two rows). The first and third rows show the neural response (mean firing rate \pm standard error on the mean, $n = 10$ trials) as a function of time. The second and fourth rows show the spike rasters. Within these rows, each panel depicts the spike activity over each of the 10 trials (rows) and time (x-axis), and are color-coded by tested body site. The vertical line labeled 'Go' indicates the start of the stimulus phase. (C) Confusion matrix of the cross-validated classification accuracy (as percentage) for predicting body parts from population neural data. Colors represent the cross-validated accuracy, as in the scale. The matrix is an average of the confusion matrices computed for each recording day individually (**Figure 1—figure supplement 3**). L: left body, ipsilateral to implant; R: right body, contralateral to implant.

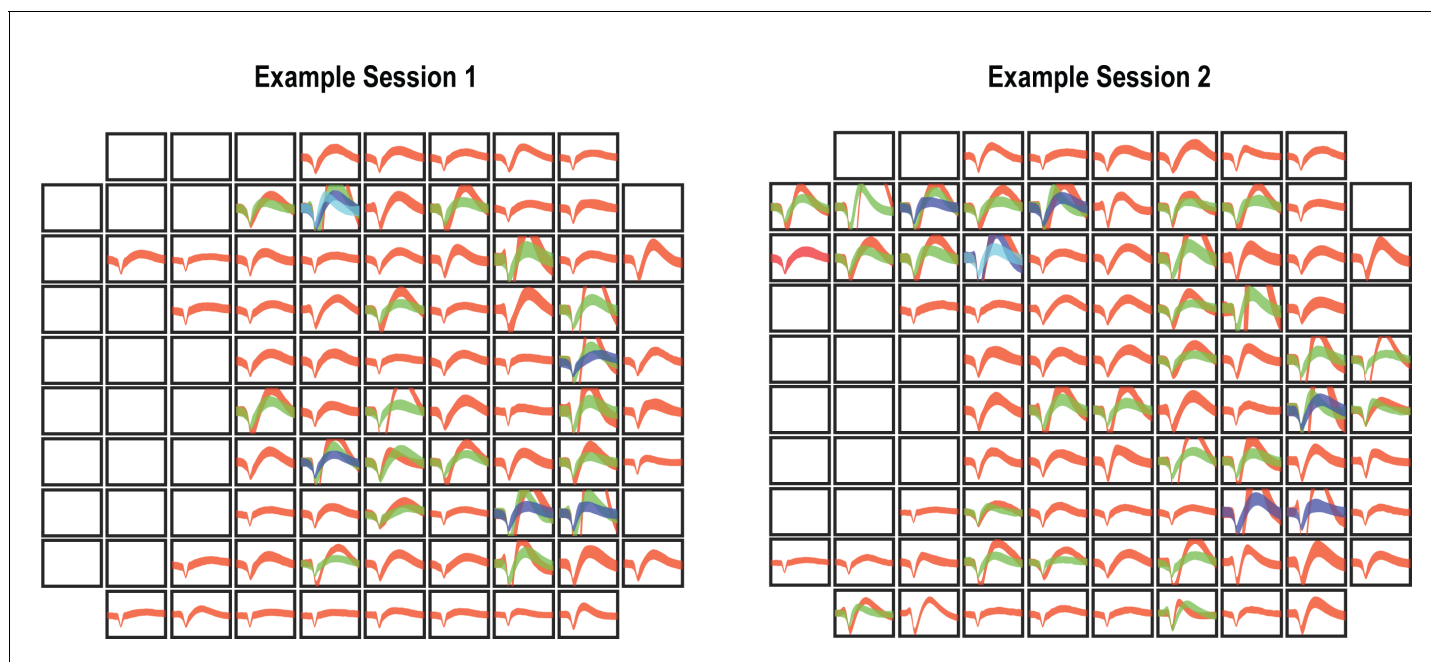


Figure 1—figure supplement 1. Nonstationary waveforms across days indicate that recorded neurons are partially distinct. We performed two analyses to quantify changes in neural recordings across days. In the first, we counted the number of waveforms on a channel and compared the number between days. If the number of waveforms changed, then this is strong evidence that there has been some substantial change in the neural recordings. By this measure, an average of $29 \pm 4.2\%$ of channels change across days. In the second analysis, we used a permutation shuffle test to measure whether the recorded waveforms on the same channel were more similar than waveforms across different channels. By this assessment, $58 \pm 8\%$ of channels change across days. These values indicate that there was some degree of neural turnover despite chronic recordings from the same implanted array. Representative changes are shown in the figure. In the two panels (left and right), the waveforms (mean \pm SD) for all sorted neurons from each spatial position on the array are shown. An empty panel indicates no evidence of neural activity. Consistent with our analysis, both the presence and/or absence of waveforms as well as their shape can vary between sessions.

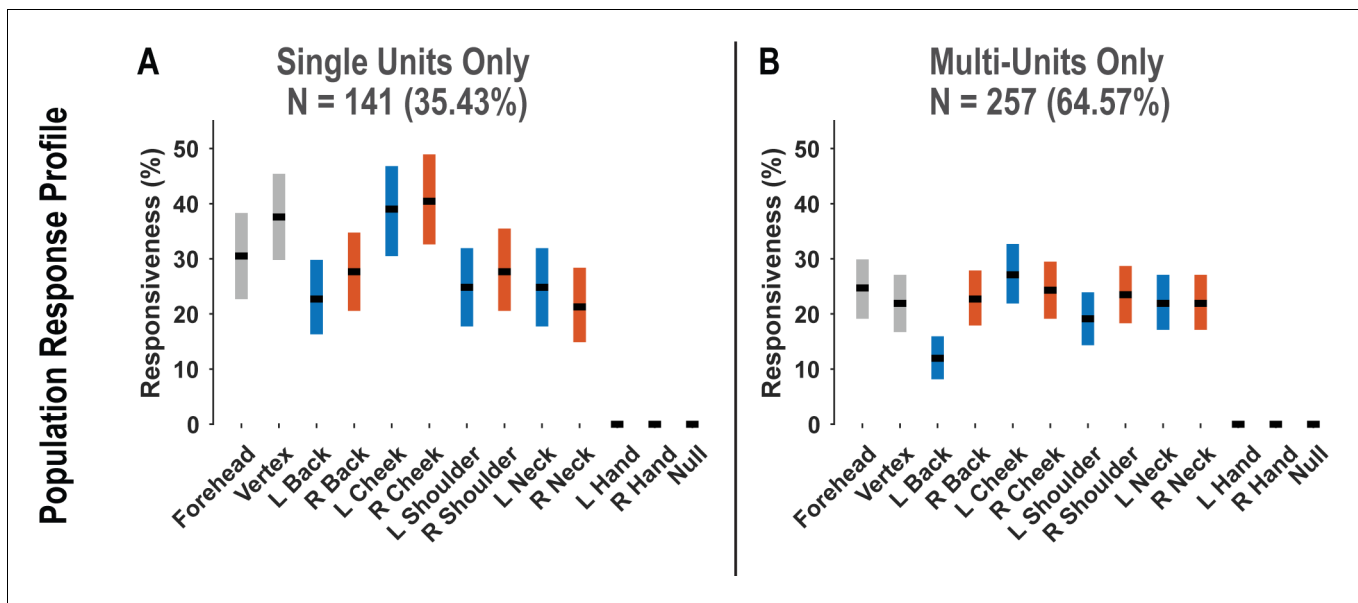


Figure 1—figure supplement 2. Postcentral-intraparietal (PC-IP) population responsiveness is not qualitatively changed by pooling together single and multi-units. (A) Percentage of the PC-IP neuronal population that demonstrated significant modulation (tuning) to each tested stimulation site ($p < 0.05$, false discovery rate corrected) when considering only high-quality single units. Within each bar, the black horizontal line represents the mean and the width of the bar represents the bootstrapped 95% confidence interval. Gray bars represent truncal (midline) body locations, blue bars represent left-sided sites, and orange bars represent right-sided sites. (B) Similar to A, but considering potential multi-units. N: sample size; L: left; R: right.

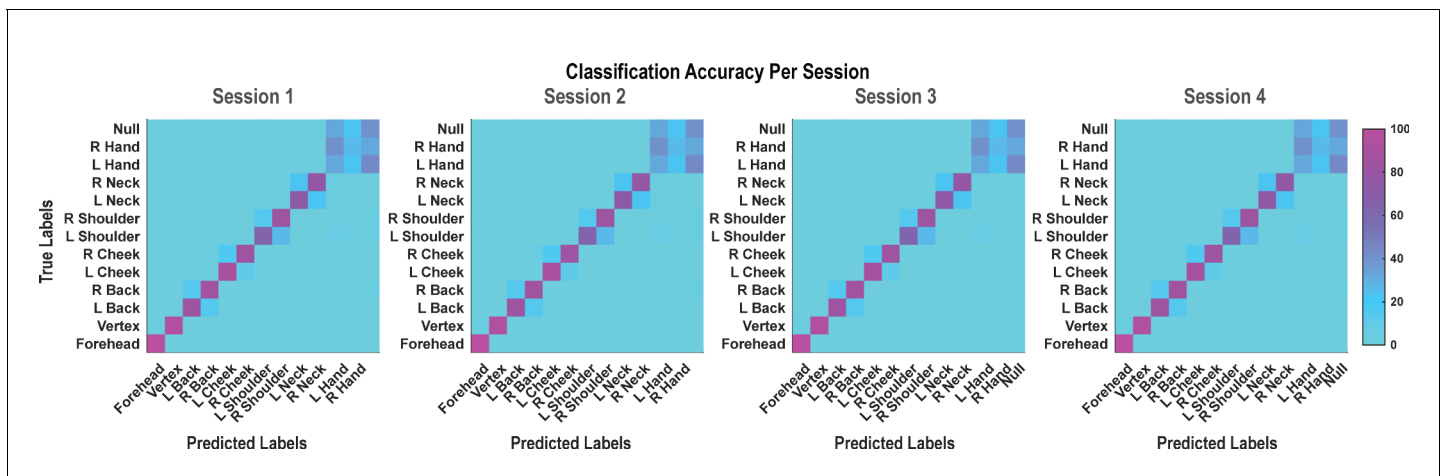


Figure 1—figure supplement 3. Population classification statistics were qualitatively unchanged between data recording sessions. Each panel from left to right represents the confusion matrix of a labeled recording session. The cross-validated classification accuracy (as percentage) in predicting actual touch conditions from population neural data is shown. These data are averaged in the matrix shown in **Figure 1C**. L: left; R, right.

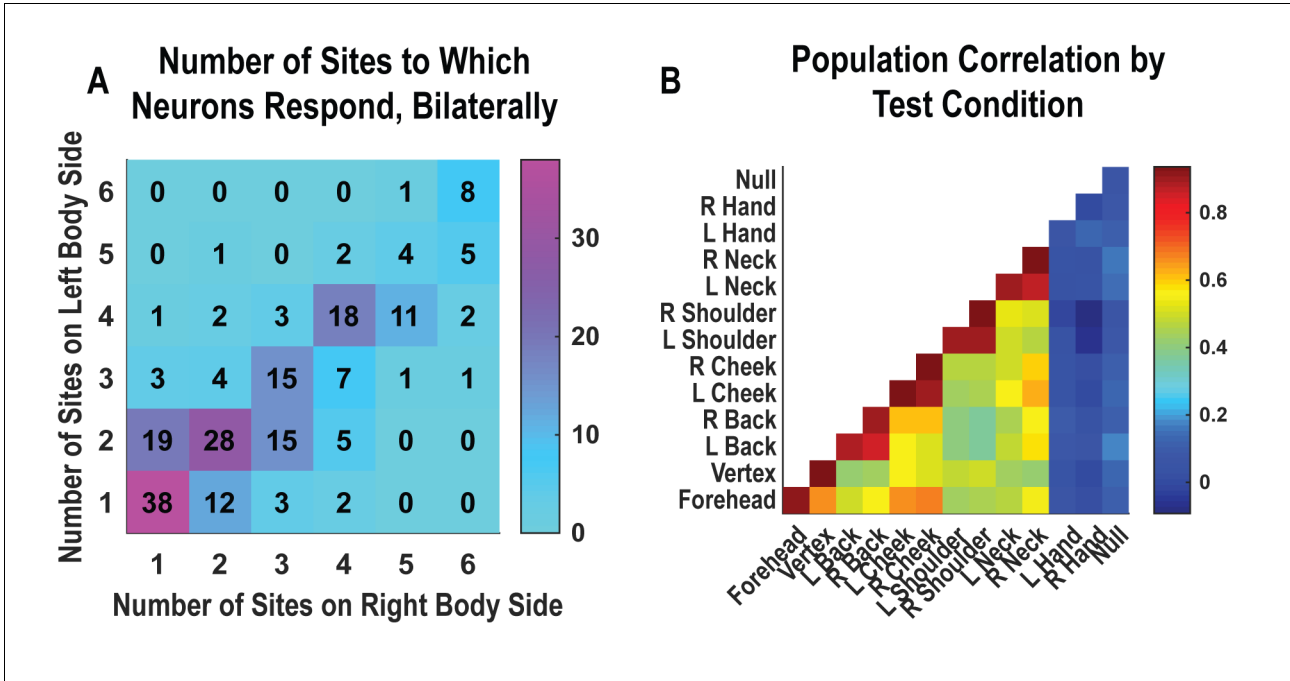


Figure 2. Neurons respond to variable numbers of bilateral receptive fields. Bilateral responses are mirror-symmetric. (A) Matrix showing the number of neurons from within the postcentral-intraparietal population that responded to the number of body parts shown, along each of the left and right body sides. Colors represent the number of neurons. Population results were not qualitatively affected by pooling together single and potential multi-units (**Figure 2—figure supplement 1**). Analysis of tactile receptive fields is shown in **Figure 2—figure supplement 2** and **Figure 2—figure supplement 3**. (B) Neuronal population correlation demonstrating the relation in encoding structure between body locations. Colors represent strength of correlation, as in the scale. Population results were not qualitatively affected by pooling together single and potential multi-units (**Figure 2—figure supplement 4**) or by choice of distance metric (**Figure 2—figure supplement 5**). For mirror-symmetry analysis at the single unit level, see **Figure 2—figure supplement 6**. L: left body, ipsilateral to implant; R: right body, contralateral to implant.

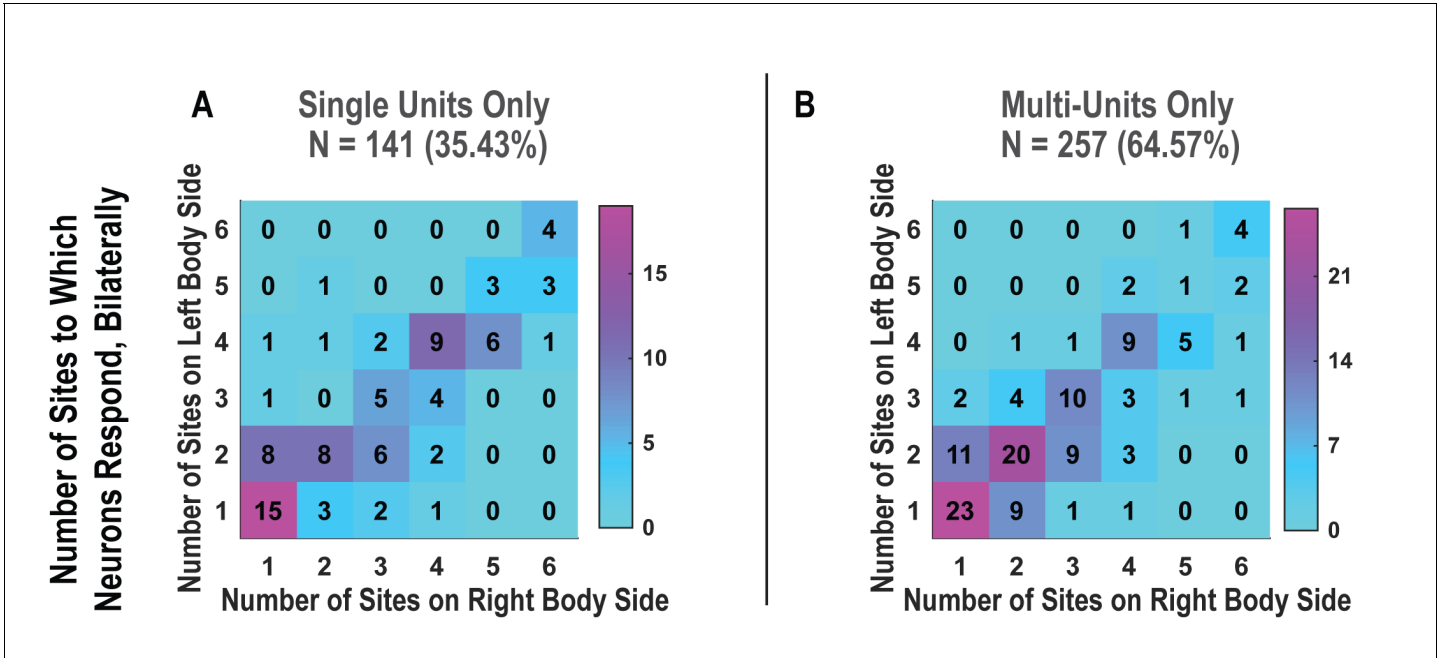


Figure 2—figure supplement 1. Bilateral responses to actual touch are not qualitatively changed by pooling together single and multi-units. (A) Matrix showing the number of neurons that responded to the number of body parts shown, along each of the left and right body sides. Only high-quality single units were considered in this matrix. The number of neurons is overlaid upon a heatmap in which the colors correspond to the number, as in the scale. (B) Similar to A, but considering potential multi-units. N: sample size; L: left; R: right.

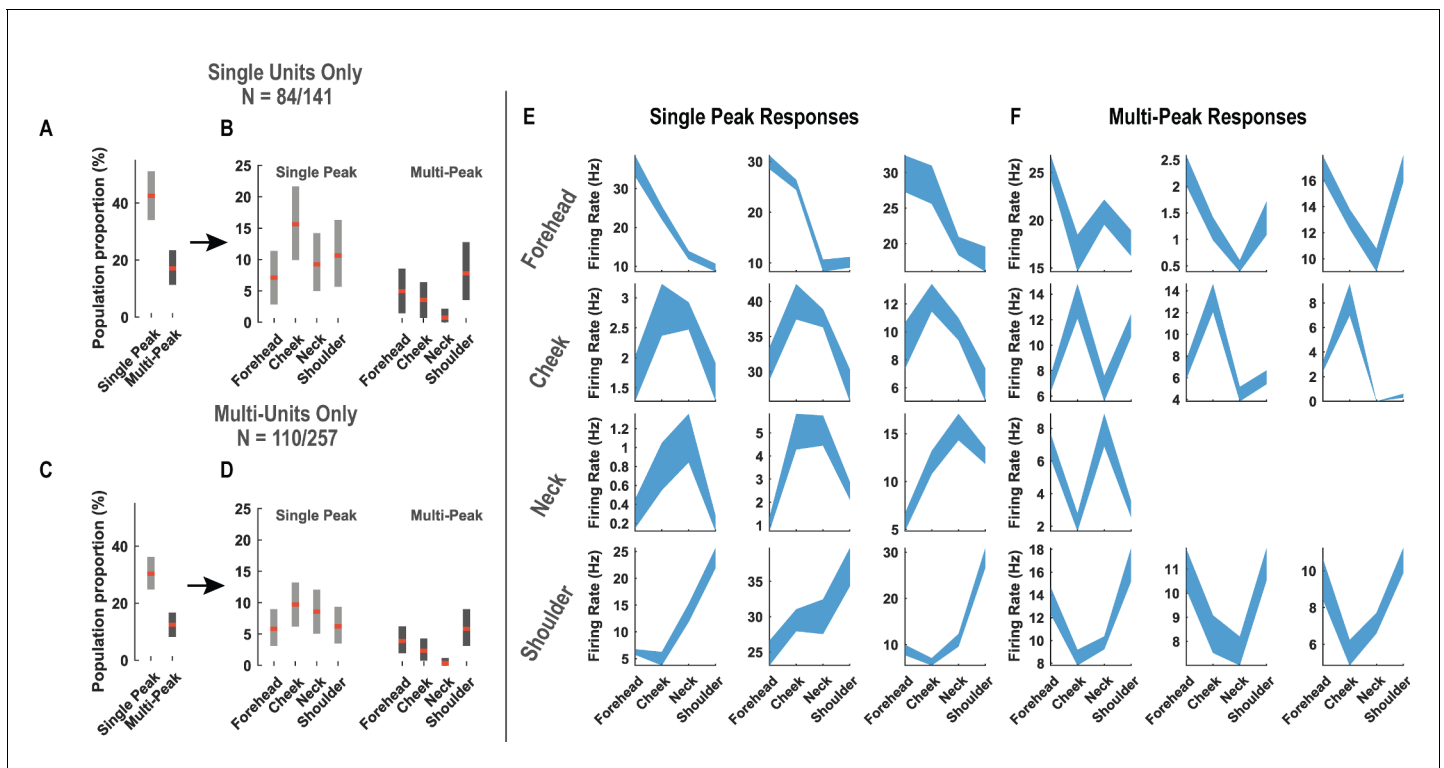


Figure 2—figure supplement 2. Diverse tactile receptive fields in human postcentral-intraparietal (PC-IP) neurons. Tactile receptive fields of PC-IP neurons were diverse with evidence both for broad single- and multi-peaked fields. Multi-peaked fields are defined as having spatially separated regions of enhanced response. (A) Percentage of neurons characterized by a broad single-peak response versus multiple peaks (mean \pm 95% CI). The analysis is described in detail in 'Materials and methods: Spatial extent of single neuron responses'. In brief, for each neuron, we found the location of maximal response and asked whether we could find a second local maxima that rose significantly above the neighboring values. If no significant second local maxima was found, the neuron was categorized as single-peak; otherwise, the neuron was categorized as multi-peak. (B) Percentage of neurons characterized by a single peak versus multiple peaks split by their preferred response field (mean \pm 95% CI). (C) Similar to A, but considering potential multi-units. (D) Similar to B, but considering potential multi-units. (E) Sample single-peak neuronal responses. Four rows depict sample units grouped according to their preferred response field (from top to bottom: forehead, cheek, neck, and shoulder). Within each panel, the neuron's firing rate (in Hertz) is depicted as a shaded blue region (the width indicating the interval from [mean - 95% CI] to [mean + 95% CI], to each of the four labeled locations). (F) Sample multi-peak neuronal responses. Conventions as in C.

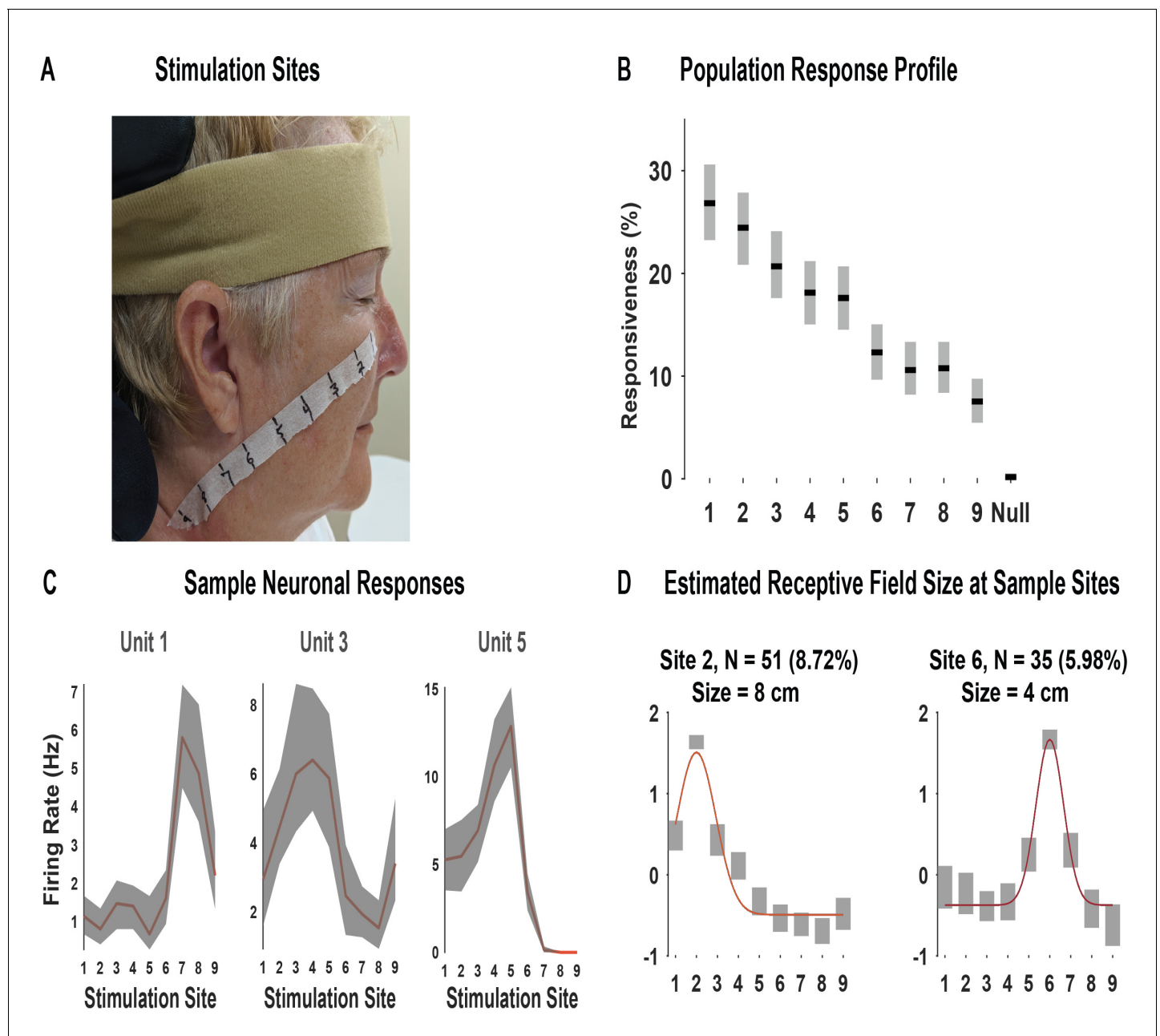


Figure 2—figure supplement 3. Receptive fields demonstrate local spatial structure. In our first experiment (**Figure 1**), we found that neurons tended to demonstrate a region of peak response with gradual reduction of the response as a function of distance with the possibility for representations at larger distances. To better understand the local parametric structure of tactile receptive fields, we performed a second experiment that tested collinear sites at finer spatial resolution. **(A)** We performed a task variant aimed at estimating the size of neuronal receptive fields to actual touch ('Materials and methods: Receptive field size'). In this variant, we tested actual touch to nine equally spaced points, 2 cm apart, along a line from the subject's cheek to her neck. This panel shows the location of stimulation points along the study subject's face and neck. Photo credit: Tyson Aflalo, California Institute of Technology. The face is masked to obscure identity per publisher's request. **(B)** Percentage of the neuronal population significantly modulated by touch to each stimulation location ($p < 0.05$, false discovery rate corrected, shown as mean \pm 95% CI, $n = 585$ units). **(C)** Representative neuronal responses showing the firing rate at each stimulation site as a function of time (mean \pm 95% CI; $n = 10$ trials). **(D)** Representative examples of neuronal responses and Gaussian fits used to estimate receptive field size (for full description, see 'Materials and methods: Receptive field size estimation'). Briefly, for each neuron demonstrating a differential response to touch to each of the nine fields, we identified the preferred site of stimulus delivery as the site associated with the largest firing rate. Next, we fit a Gaussian model to the average responses at the nine sites, with the mean/center of the model fixed at the preferred response site. The receptive field size was estimated as the full width at half maximum. In each of the examples depicted, the colored lines represent the Gaussian model fit to the average responses. The number of units included in the

Figure 2—figure supplement 3 continued on next page

Figure 2—figure supplement 3 continued

analysis for each example site is indicated in the title of each subplot (as both the absolute number of neurons and as a percentage of the recorded neuronal population). The receptive field size was described as the full width at half maximum, shown in the title of each subplot. In each subplot, the x-axis indicates the stimulation site. The y-axis is a standard (z) score. Hz: Hertz; cm: centimeter.

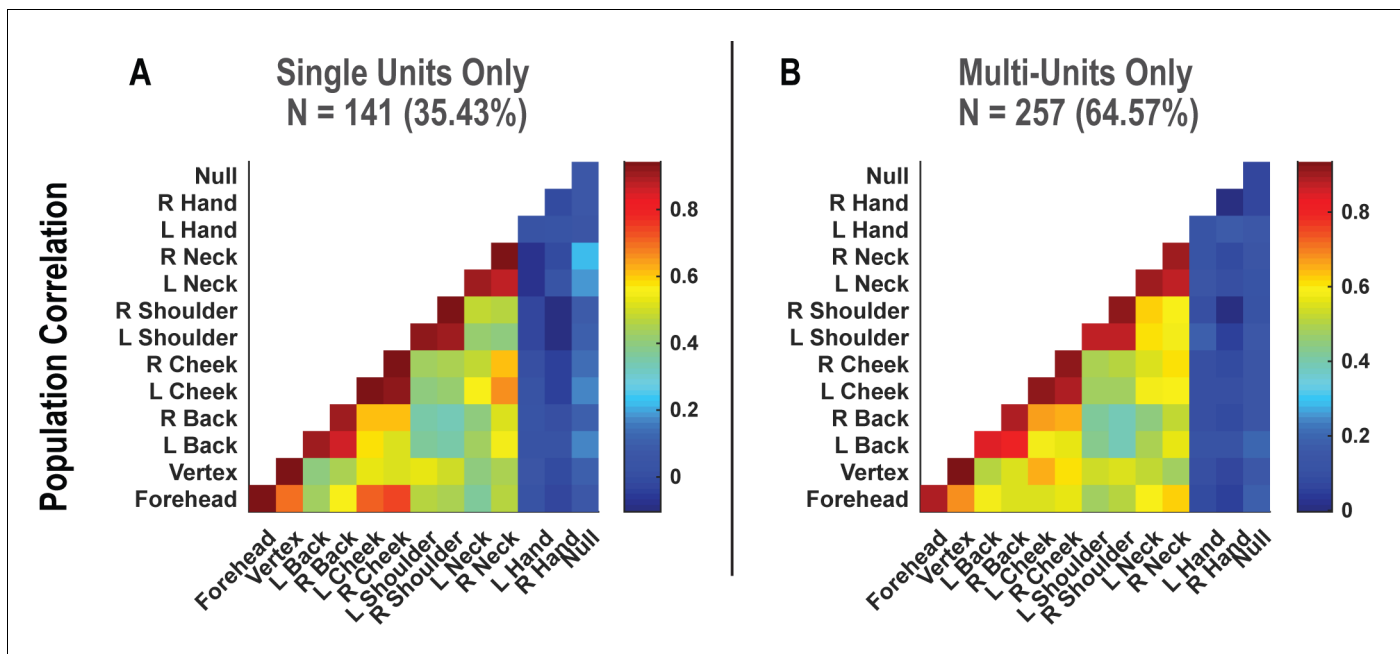


Figure 2—figure supplement 4. Symmetry in population-level responses to bilateral touch is not qualitatively changed by pooling together single and multi-units. (A) Population correlation demonstrating the relation in encoding structure between test conditions, when considering only high-quality single units. Colors represent the strength of correlation, as in the scale. (B) Similar to A, but considering potential multi-units. N: sample size; L: left; R: right.

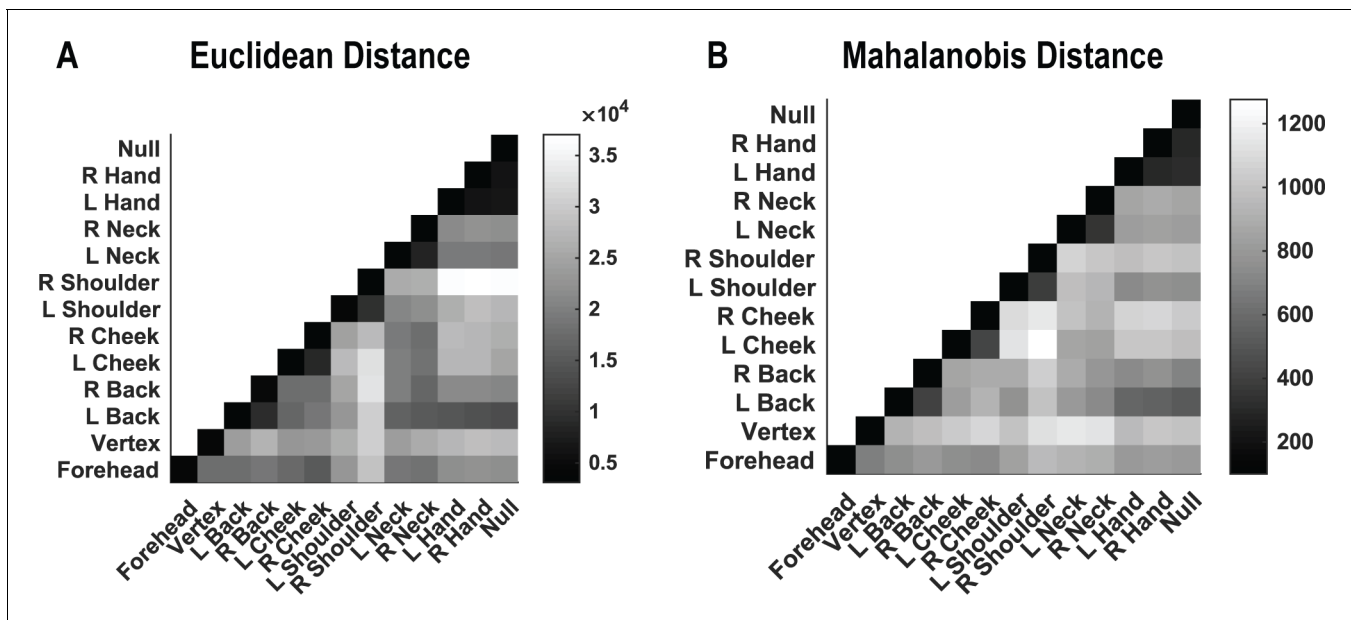


Figure 2—figure supplement 5. Relationships of population responses to touch are conserved across distance metrics. (A) Population similarity in encoding structure (for correlation data presented in **Figure 2B**) between test conditions when evaluated by Euclidean separation. Colors represent the distance, as in the scale. (B) Population similarity in encoding structure (for the same data as in A) between test conditions when evaluated by Mahalanobis separation. Colors represent the distance, as in the scale. L: Left; R: right.

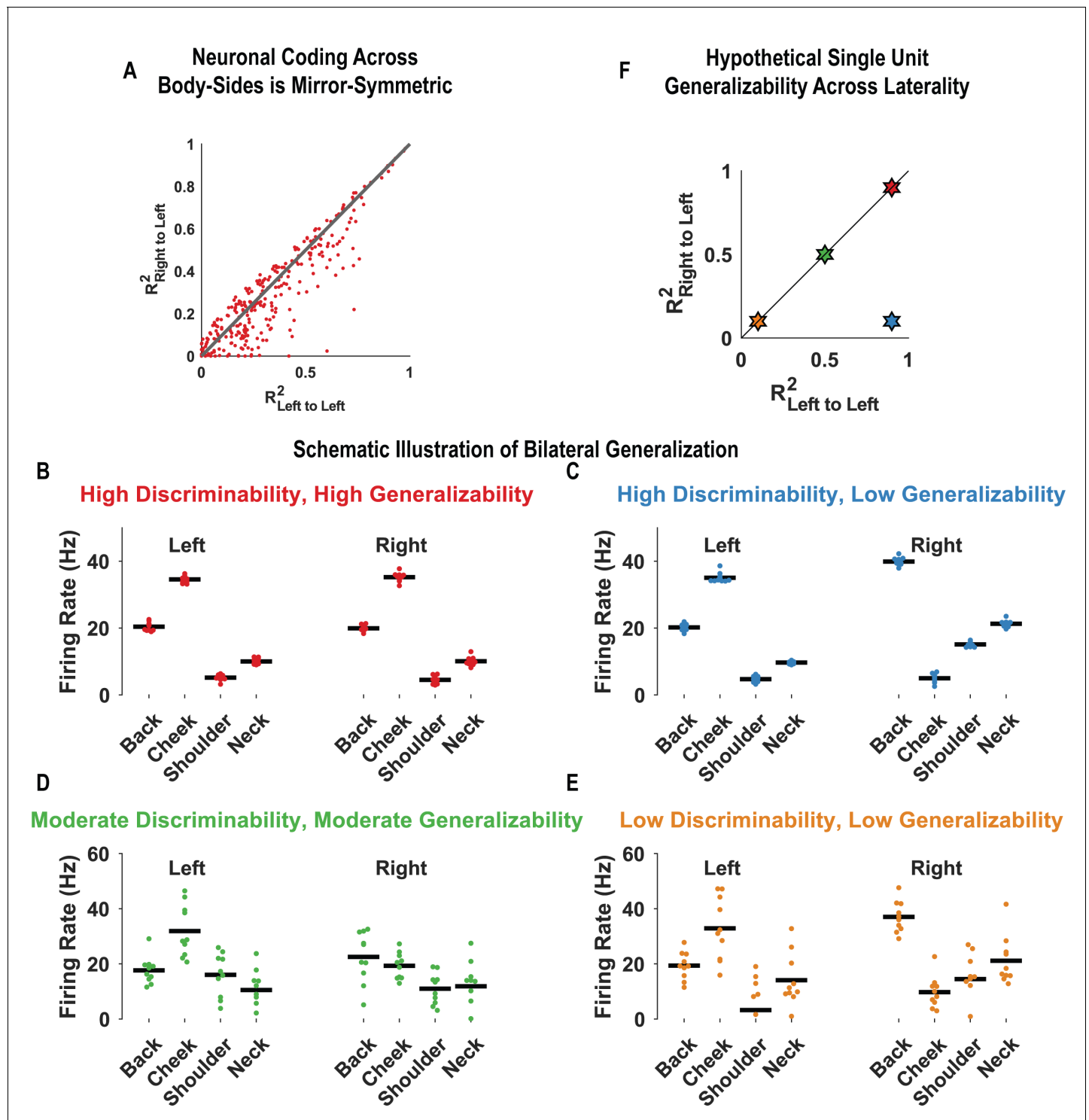


Figure 2—figure supplement 6. The majority of postcentral-intraparietal neurons code tactile receptive fields bilaterally in a mirror-symmetric manner. We evaluated mirror-symmetric bilateral coding at the level of single neurons. We used the same basic procedure as the population case (**Figure 2B**), although in the single-unit case, cross-validated comparisons were done per-unit. All neurons demonstrating significant modulation from baseline for at least one location (263 of 398 units; 66.1%) were included in this analysis. (**A**) Scatter plot comparing the consistency in touch responses to the same body side against responses across body sides. Units close to the identity line code the left and right sides with the same pattern of activity and thus in a mirror-symmetric fashion (see ‘Materials and methods: Tests for mirror-symmetric neural coding of body locations: single-unit analysis’). The analysis used in this plot is depicted schematically in **B–E**. (**B**) Firing rate for an example unit over 10 trials (red dots) is shown, to touch to each indicated body part (both left and right). The black horizontal line indicates the mean response. The variance in trial-by-trial responses to each body part within a body

Figure 2—figure supplement 6 continued on next page

Figure 2—figure supplement 6 continued

side is low (i.e., high discriminability). Moreover, the pattern of responses on the left and right sides is closely matched (i.e., the encoding is highly generalizable across sides). (C) Conventions are as in B. In this panel, the firing rate of a unit over 10 trials (blue dots) is shown. As in B, the variance in trial-by-trial responses within each body side is low (i.e., high discriminability). However, the patterns of responses on the left and right sides are dissimilar (i.e., the encoding is poorly generalizable across sides). (D) Conventions are as in B. Green dots represent the trial responses to touch. The inter-trial variance in responses is larger than that in the top two panels (i.e., moderate discriminability). The pattern of responses between the left and right sides is moderately matched (i.e., moderate generalizability). (E) Conventions as in B. In this panel, the yellow dots represent trial responses that have a high variance (i.e., low discriminability) and are also poorly matched in patterns between the left and right sides (i.e., low generalizability). (F) Scatter plot showing four illustrative neurons. These are color-coded as in B–E and demonstrate how neurons with similar and dissimilar patterns of encoding will be arranged when their corresponding strength of encoding within a body side ($R^2_{\text{Left to Left}}$) is compared to how well one side generalized to the other body side ($R^2_{\text{Right to Left}}$).

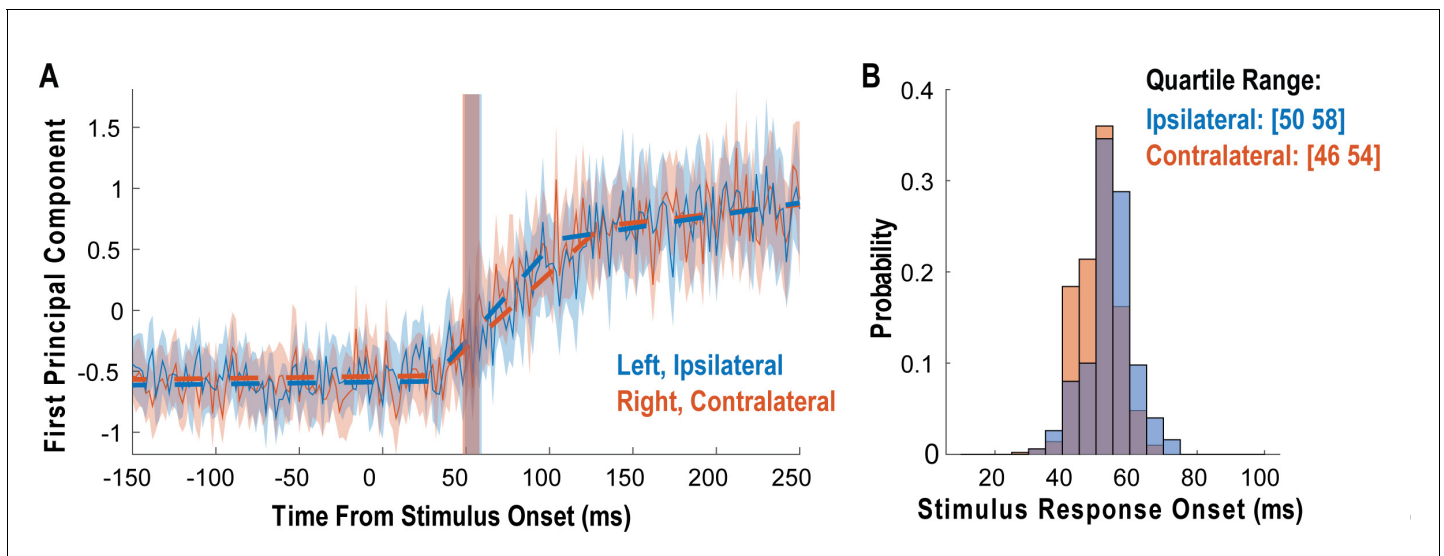


Figure 3. Tactile responses occur at short latency. (A) Population response was quantified as the first principal component (mean \pm 95% CI). Population response was computed separately for the left (blue; ipsilateral to implant) and right body sides (orange; contralateral to implant) and is shown as a function of time (2 ms window size, 2 ms step size, no smoothing). Dashed lines show piecewise linear fit used to compute latency. Transparent vertical bar shows inter-quartile latency range based on a bootstrap procedure (see B). (B) Distribution illustrating variability of latency estimates for the recorded data using a bootstrap procedure. Color code as in A.

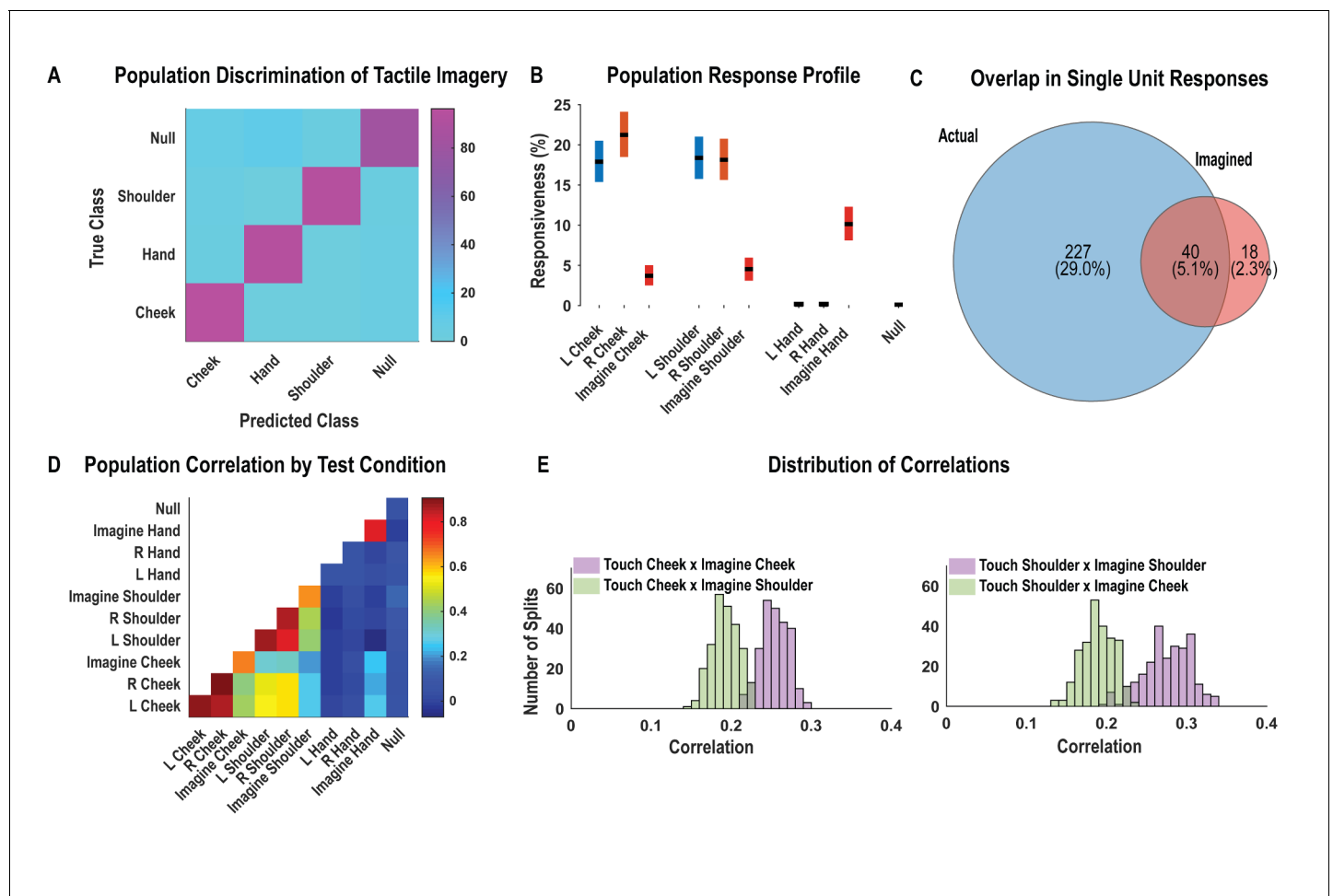


Figure 4. Postcentral-intraparietal (PC-IP) neurons encode body part-specific responses during the tactile imagery task. (A) Average classification confusion matrix across recording sessions for body parts during tactile imagery and the baseline (null) condition. Colors represent prediction accuracy as a percentage, as in the scale. (B) Percentage of PC-IP neurons significantly modulated from baseline (mean \pm 95% CI, $p < 0.05$, false discovery rate corrected, $n = 838$ units) split by test condition. Population results were not qualitatively affected by pooling together single and potential multi-units (Figure 4—figure supplement 1). (C) Venn diagram illustrating the number (percentage) of PC-IP neurons recorded that activated during actual and imagined touch, and their overlap. (D) Population correlation matrix depicting similarity of the population response between all test conditions. Colors represent the correlation strength, as in the scale. (E) Distribution of correlations between actual shoulder (left) and cheek (right) touch and imagined cheek/shoulder touches, with the distributions computed over different splits of the data (see ‘Materials and methods: Population correlation’). L: left body, ipsilateral to implant; R: right body, contralateral to implant.

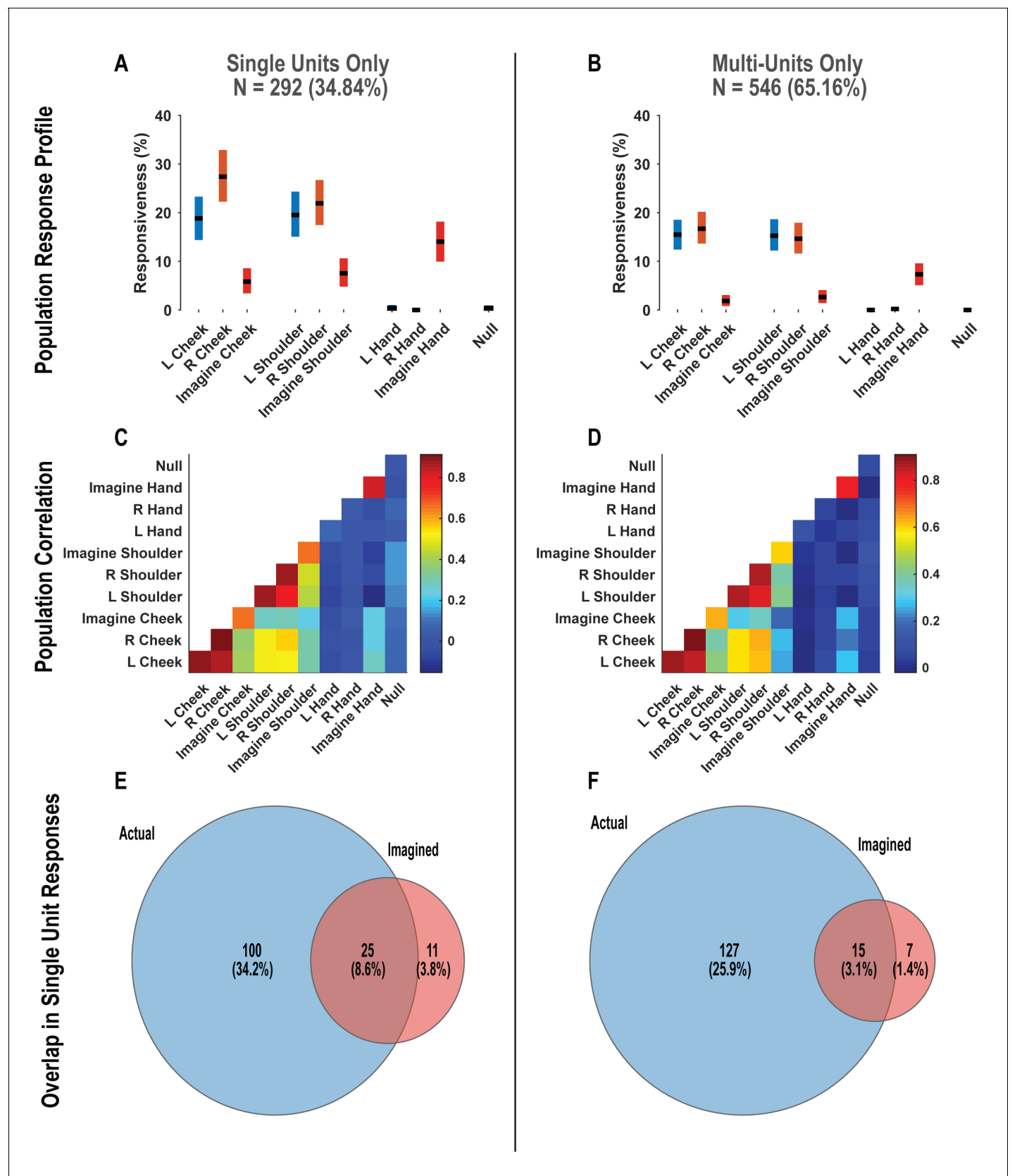


Figure 4—figure supplement 1. Postcentral-intraparietal (PC-IP) responses during the tactile imagery task are not qualitatively changed by pooling together single and multi-units. (A) Percentage of the PC-IP neuronal population that demonstrated significant modulation (tuning) to each tested stimulus. Figure 4—figure supplement 1 continued on next page

Figure 4—figure supplement 1 continued

stimulation site ($p < 0.05$, false discovery rate corrected) when considering only high-quality single units. Within each bar, the black horizontal line represents the mean and the height of the bar represents the bootstrapped 95% CI. Blue bars represent actual touch to left-sided sites, orange bars represent actual touch to right-sided sites, and red bars represent imagined touch (to right-sided sites). **(B)** Similar to **A**, but considering potential multi-units. **(C)** Population correlation demonstrating the relation in encoding structure between test conditions when considering only high-quality single units. Colors represent the strength of correlation, as in the scale. **(D)** Similar to **C**, but considering potential multi-units. **(E)** Venn diagram illustrating the number (percentage) of PC-IP neurons recorded that activated during actual and imagined touch, and their overlap, when considering only high-quality single units. **(F)** Similar to **E**, but considering potential multi-units. N: sample size; L, left; R, right.

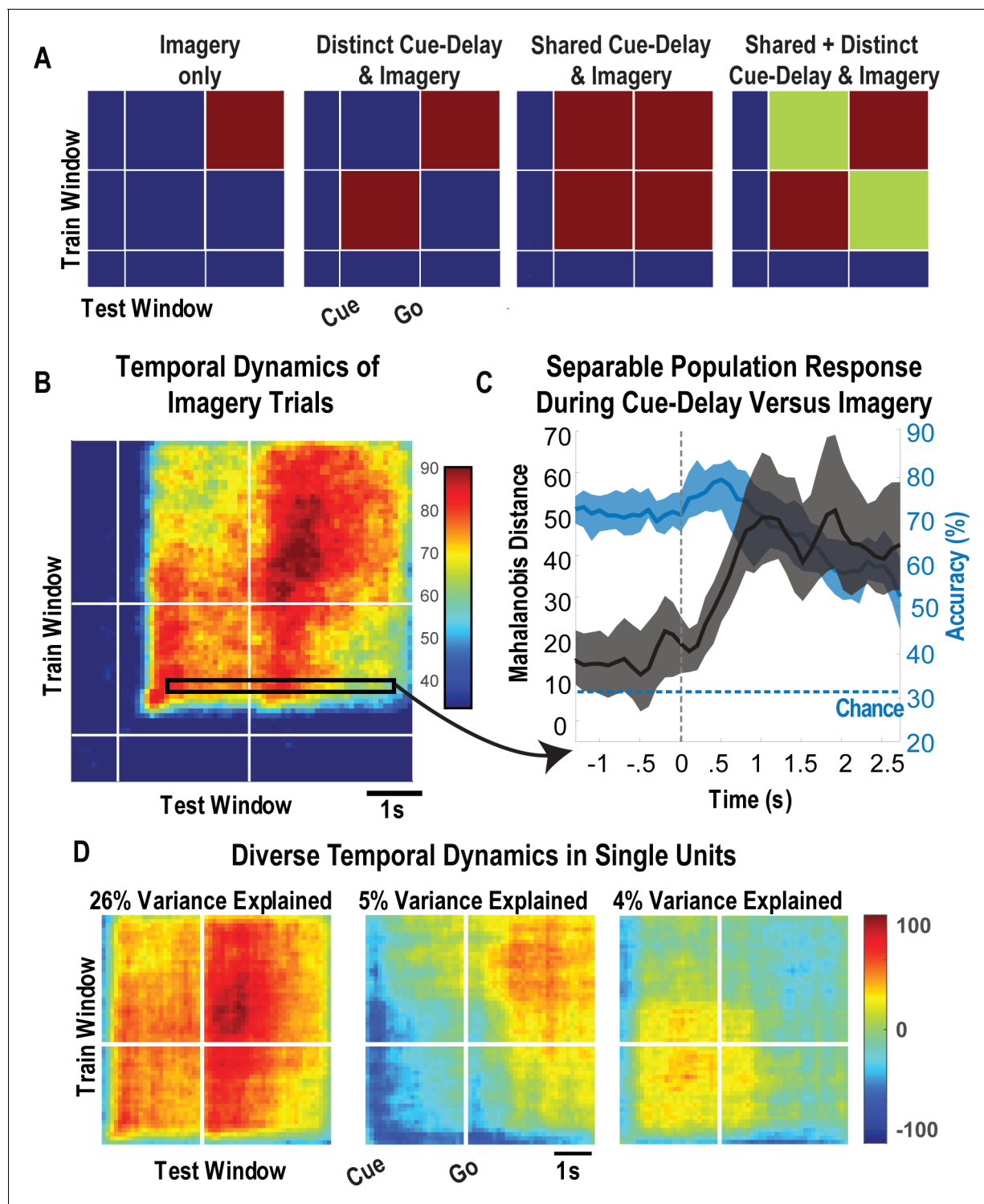


Figure 5. Shared and distinct coding of body parts during cue-delay and imagery epochs. (A) Schematic illustrating possible dynamic classification patterns over epochs of the tactile imagery task. In each panel, the window used for classifier training is along the y-axis and the window used for classifier testing is along the x-axis. The start of the auditory cue (marking the onset of the cue-delay epoch) and the beep (marking the go signal for the imagery epoch) is shown as solid white lines, labeled 'Cue' and 'Go.' (B) Dynamic classification analysis results for the imagined touch test conditions with conventions as in A. The colors represent prediction accuracy values (as percentage), as in the scale. (C) Illustration of distinct and shared neuronal responses between the cue/delay and imagery epochs for the boxed window of B. Shared response illustrated with cross-validated, classification generalization accuracy (blue, mean with 95% confidence interval computed across sessions). Distinct response illustrated with cross-

Figure 5 continued on next page

Figure 5 continued

validated Mahalanobis distance (gray, mean with 95% confidence interval computed across sessions). The dashed vertical line marks the onset of the imagery epoch. The dashed horizontal line marks chance classification accuracy. **(D)** Dynamic classification matrices were constructed separately for all selective units. The first three principal components (PCs) of the dynamic classification matrices of single-unit activity are shown, along with the fractional variance explained by each. The mean activity of all neurons within the PC is shown within each panel, color-coded by PC weights. Plot conventions are as in **A** and **B**. s: seconds.

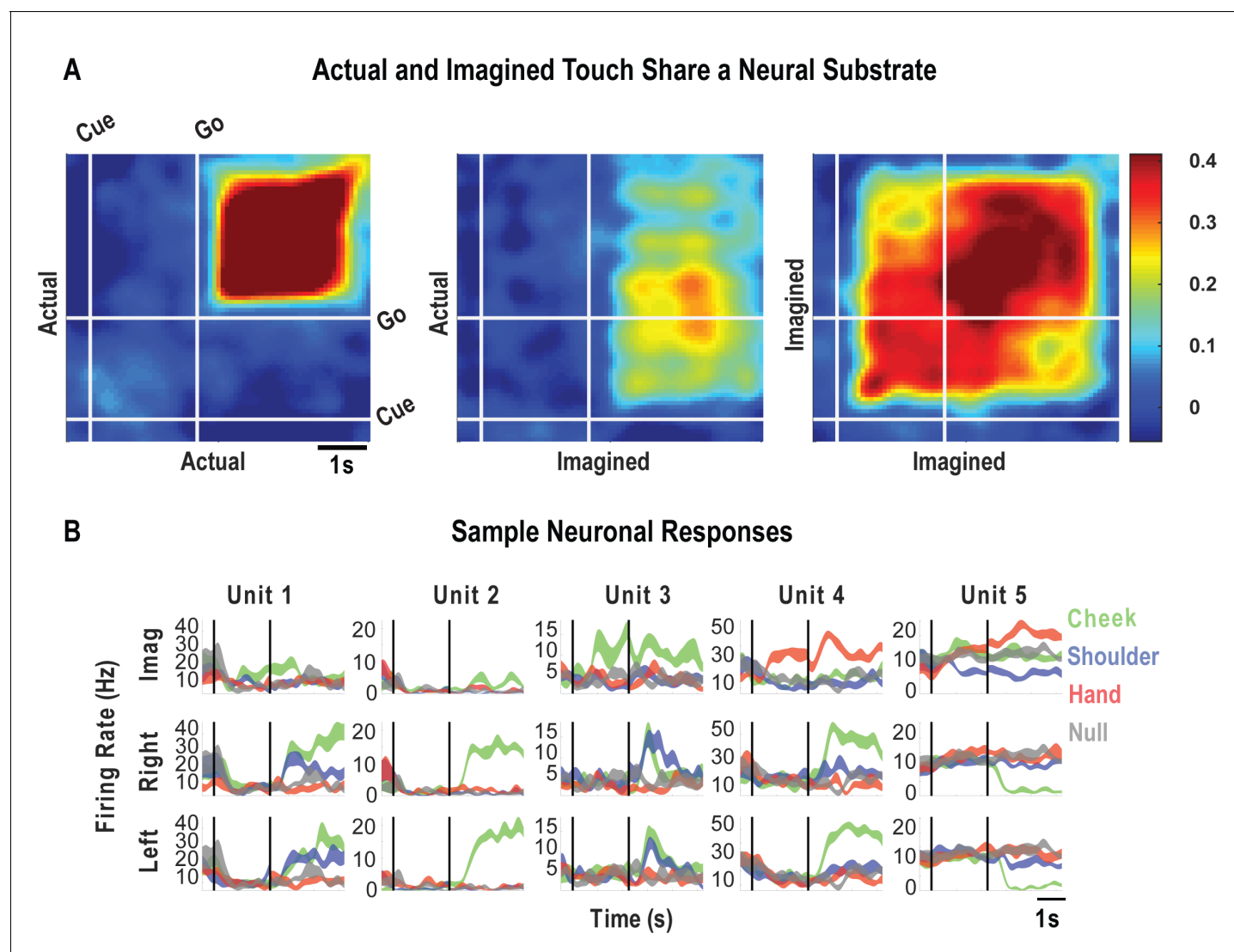


Figure 6. Cue-delay and imagery-evoked neural activity shares a neural substrate with actual touch. (A) Within- and across-condition dynamic, cross-validated correlation analysis demonstrating a shared neural substrate between imagined and actual tactile sensations. Each panel shows how the neural population response at one slice of time compares to all other slices of time for the two formats being compared (x- and y-axis labels). Correlation magnitude is indicated by color as in the bar. The start of the auditory cue (marking the onset of the cue-delay epoch) and the beep (marking the go signal for the imagery epoch) is shown as solid white lines, labeled 'Cue' and 'Go.' (B) Representative neuronal responses illustrating selectivity during actual and imagined sensations. Each panel shows the firing rate (in Hertz, mean \pm SEM) through time (vertical lines signal onset of cue/delay and go phases as labeled). Each column illustrates the responses of the same unit to tactile imagery of the right side (top), actual touch on the right side (middle), and actual touch on the left side (bottom) for matched body parts.